Vol 14 No 7, July 2005
1009-1963/2005/14(07)/1465-06

Chinese Physics

© 2005 Chin. Phys. Soc.
and IOP Publishing Ltd

Incident angle dependence of secondary electron emission from carbon induced by swift H_2^+

Lu Qi-Liang(卢其亮)[a)b)†], Zhou Zhu-Ying(周筑颖)[b)],
Shi Li-Qun(施立群)[b)], and Zhao Guo-Qing(赵国庆)[b]

[a)] *National Laboratory of Solid State Microstructures and Department of Physics, Nanjing University, Nanjing 210093, China*

[b)] *Applied Ion Beam Physics Laboratory, Institute of Modern Physics, Fudan University, Shanghai 200433, China*

(Received 12 July 2004; revised manuscript received 4 March 2005)

The incident angle dependence of secondary electron emission induced by a swift H_2^+ ion impinging on carbon is studied using the Monte Carlo method combined with the semiempirical theory. The relationships both between the electron emission yield and the project angle and between the statistics and the projectile angle are investigated. The results show that the backward electron emission yield deviates from the inverse cosine law, due to the effect of the valence electrons of H_2^+. The ratio of the forward electron emission yield to the backward electron emission yield at the inclining incidence is different from that at the normal incidence. The statistical distribution of electron emission is independent of the incident angle. The value of b, the deviation parameter from the Poisson distribution, increases with projectile energy.

Keywords: secondary electron emission, incidence angle, Monte-Carlo simulation, valence electron, statistical distribution

PACC: 7900, 3450D

1. Introduction

Ion induced secondary electron emission is an important result of interactions between ion and the surface of a solid, which could be utilized for the design of particle detectors. The extensive attention has been drawn to its theoretical and experimental studies. In general, the projectile is normally incident on the solid surfaces at the incident angle $\theta = 0$. With the increase of θ, the geometrical pathlength of the projectile within the escape zone of secondary electron is prolonged by a factor of $\cos^{-1}\theta$. If we assume that the path of ion in the solid is straight and the energy deposition over the pathlength within the escape zone is constant, the expected total electron yield is

$$Y(\theta) = Y(0)\cos^{-1}\theta. \tag{1}$$

For heavy ion impact, deviations from formula (1) have been found.[1−11] These authors found that the experimental result for $\theta < 60^\circ$ could be fitted by an empirical formula:

$$Y(\theta) = Y(0)\cos^{-f}\theta, \tag{2}$$

where f is a parameter in the range $0.5 \leq f \leq 1.5$.

In these references, except Ref.[10], the velocity of ions rather than protons is generally lower than the Bohr velocity, and the projectiles are atomic ions. When a swift H_2^+ molecular ion with energy E_0 impinges on a solid, only a few collisions are required to strip a valence electron from the projectile. Then H_2^+ becomes an H^+-ion -pair and e^-. The residual ionic fragments recede from one another under the influence of the interionic Coulomb force. Due to the interference in electronic excitation of the target induced by the atomic ions contained in the projectile molecular ion, the action of H_2^+ is far more complex than that of a simple H^+ ion in the solid. The stopping power of H_2^+ is significantly different from that of separated H atomic ions. This is usually called the "vicinage effect". Accordingly, secondary electron emission yield induced by H_2^+ also differs from that induced by the

†E-mail:qllufd@vip.sina.com

monatomic H^+. In this work, a Monte Carlo simulation code for the kinetic electron emission from carbon is developed. The incident angle dependence of secondary electron emission induced by swift H_2^+ ion is studied.

2. Backward electron emission induced by H_2^+

The yield of backward electrons for a given incident angle and pathlength of x can be described as follows:

$$Y_{\rm b} = Y_{\rm b}(\infty,\theta)(1-{\rm e}^{-x\cos\theta/\lambda_{\rm s}}), \tag{3}$$

where $Y_{\rm b}(\infty,\theta)$ represents the backward yield for the pathlength $x\to\infty$, and $\lambda_{\rm s}$ is the characteristic diffusion length for low energy electrons. So the differential form of Eq.(3) is

$${\rm d}Y_{\rm b} = \frac{Y_{\rm b}(\infty,\theta)}{\lambda_{\rm s}}{\rm e}^{-x\cos\theta/\lambda_{\rm s}}{\rm d}x, \tag{4}$$

which represents the number of backward secondary electrons coming from a depth between x and $x+{\rm d}x$.

The main processes for H_2^+ ions incident on the solids are H_2^+ ions with the effective charge $Z_{\rm eff1}$ travelling in solids (here $Z_{\rm eff1}$ can be calculated according to Ref.[12]), and H_2^+ ions splitting into H^+-ion-pairs (H^++H^+) and e^- at a depth greater than $\lambda_0(E_0)$. $\lambda_0(E_0)$ is the electron loss mean free path of H_2^+, and can be obtained from the fitting of results in Ref.[13]. We assume that the electron is stripped from H^0. So the electron emission yield for H_2^+ impact is explained by considering three contributions: the yield Y_1 induced by an H_2^+ ion, the yield Y_2 by an (H^++H^+)-ion-pair and the yield $Y_{\rm e}$ by a stripped electron with the same velocity. The yield for H_2^+ is given by

$${\rm d}Y_{\rm b} = p(x)dY_1 + (1-p(x))({\rm d}Y_2+{\rm d}Y_{\rm e}), \tag{5}$$

which was originally used to calculate the electron yield induced by neutral hydrogen atoms in Ref.[14], where $p(x)=\exp(-x/\lambda_0)$. By integrating Eq.(4) over the whole target thickness, we obtain

$$\begin{aligned} Y_{\rm b} =& \frac{\lambda_0\cos\theta}{\lambda_0\cos\theta+\lambda_{\rm s}}Y_1 \\ &+\left(1-\frac{\lambda_0\cos\theta}{\lambda_0\cos\theta+\lambda_{\rm s}}\right)(Y_2+Y_{\rm e}). \end{aligned} \tag{6}$$

For swift light ions, such as H^+ and He^+, Eq.(1) holds strictly.[2,4,8,9] According to the theory in Ref.[15], the electron yield is proportional to the electronic stopping power S of ion near the surface at normal incidence, $Y_b(0)=\Lambda S$. So Y_1 and Y_2 can be written as

$$Y_i(\theta) = \Lambda\frac{S_i}{\cos\theta}, \quad i=1,2, \tag{7}$$

where Λ depends on the target material. while

$$S = Z_{\rm eff}^2 S_{\rm p} \tag{8}$$

is the stopping power of ions with the effective charge $Z_{\rm eff}$, and $S_{\rm p}$ is the stopping power of protons with the same velocity and can be calculated with TRIM96.[16] So the stopping power of H_2^+ is $S_1 = Z_{\rm eff1}^2 S_{\rm p}$. Due to the "vicinage effect", the H^+-ion-pair should be treated as a point-charge-pair. The stopping power of (H^++H^+) can be written as

$$S_2 = Z_{\rm eff2}^2 S_{\rm p}. \tag{9}$$

Here, $Z_{\rm eff2} = (Z_1^{*2}+Z_2^{*2}+2Z_1^*Z_2^*g(r))^{1/2}$,[17] Z_1^* and Z_2^* are the effective charges of the atomic ions. $g(r)$ is the vicinage function and r is the internuclear distance. For (H^++H^+) ion-pairs,

$$\begin{aligned} Z_1^* = Z_2^* =& [(1-\exp(-75E_0)) \\ &\times\exp(-0.835\exp(-7.25E_0))]^{1/2}, \end{aligned} \tag{10}$$

where E_0 is in units of MeV. A detailed explanation of $g(r)$ can be found in Ref.[17]. According to this reference,

$$r = (1+0.235857(x/D_0))^{1.6473}r_0, \tag{11}$$

where x is the depth of ion cluster in the solid, r_0=0.129nm[18] is the initial internuclear distance of H_2^+, and $D_0 = v_0(\mu r_0^3/2Z_1^*Z_2^*e^2)^{1/2}$, in which $\mu = M_1M_2/(M_1+M_2)$ is the reduced mass, v_0 is the projectile velocity, and M_1, M_2 are the mass of the component ions of (H^++H^+). The stripped electron can be viewed as a primary projectile electron, so $Y_{\rm e}$ is the sum of secondary electron emission yield γ and backscatter coefficient η. γ can be taken from Ref.[19] as follows:

$$\gamma = 2.72^2 Y_{\rm m}(E/E_{\rm m})\exp[-2(E/E_{\rm m})^{1/2}], \tag{12}$$

where E is the energy of electron, $Y_{\rm m}=0.9$ is the maximum yield and $E_{\rm m}$=350eV is the corresponding incident energy.[20] We choose the backscatter coefficient $\eta=0.15$.[14] According to the Refs.[21] and [22], the relationship between the electron yield and incident angle is $Y_{\rm e}(\theta) = Y_{\rm e}(0)\cos^{-f}\theta$, where f=0.6 is taken.

3. Monte Carlo Simulation

The Monte Carlo method is widely used to simulate the electron emission induced by ions[23−25] and the transport of electrons in a solid.[26,27] Recently, a Monte Carlo simulation code for calculating the electron emission from carbon induced by H_2^+ ions has been developed in our laboratory. The basic concept of the Monte Carlo model of the kinetic electron emission is to simulate the trajectories of the projectile particles penetrating into the solid and those of excited kinetic electrons travelling towards the surface with a given cross section for active scattering processes. Particle travelling trajectories in solids are assumed to be straight lines between the sites of interactions. For the transport of incident ions in the target, the elastic collisions are treated with the formula in Ref.[28]. The main processes for H_2^+ incident on the solids are H_2^+ ions with the effective charge $Z_{\rm eff1}$ travelling in solids, and H_2^+ splitting into H^+ ion-pair (H^++H^+) and e^- at a depth greater than $\lambda_0(E_0)$.

In general, according to the free electron gas model, the electronic structure of the solid is composed of inner shell electrons at discrete energy levels and electrons in a single conduction band. The charged projectile can excite electrons from the conduction band or from the inner shell of the target atoms. The electrons excited by projectiles undergo elastic and inelastic collisions in the target, and then generate cascade electrons. The moving electrons are traced until they possibly leave the target or until their energies drop below a certain energy level, and then they stay in the target. The detailed description of the simulation code can be seen in Ref.[29]. In particular, The elastic cross-sections of the electrons with momentum p and speed v are calculated using the screened Rutherford formula with a correction factor adopted in Ref.[30] based on cross-section calculations from a partial wave analysis. Cross-section values at the energies not tabulated in Ref.[30] can be obtained by interpolating and extrapolating the values from the table. In the Monte Carlo calculations conducted here 10000 projectile H_2^+ ions are traced. The density parameter $r_{\rm s}$ of the electron gas of carbon used here is 1.65. The target thickness for inclining incidence is 50nm.

4. Dependance of electron emission yield on incident angle θ

Due to lack of the experimental results about incident angle dependence of secondary electron emission from carbon induced by swift H_2^+, the calculated results can be compared only with the measurements at normal incidence.[31] The ratio of the forward electron yield to the backward one, $Y_{\rm f}/Y_{\rm b}$, as a function of target thickness is shown in Fig.1. A reduced ratio R of the emission yield for molecular ions $Y(H_2^+)$ to that for protons $Y(H^+)$ is defined as $R = Y(H_2^+)/2\,Y(H^+)$. The relationship between $R(Y_{\rm f})$ and target thickness is shown in Fig.2. The experimental results are well reproduced by our theoretical calculation. In Figs.1 and 2, the calculations are slightly larger than measurements. The reason may be that the actually increasing rate of internuclear distance r with the depth of H^++H^+ ion clusters in the solid is faster than that obtained from Eq.(11). Therefore, we overestimate the effective charge of (H^++H^+)-ion-pairs. Nevertheless, the simulation results prove that the basic theoretical assumption made in the present work has already provided a description for the most relevant process involved.

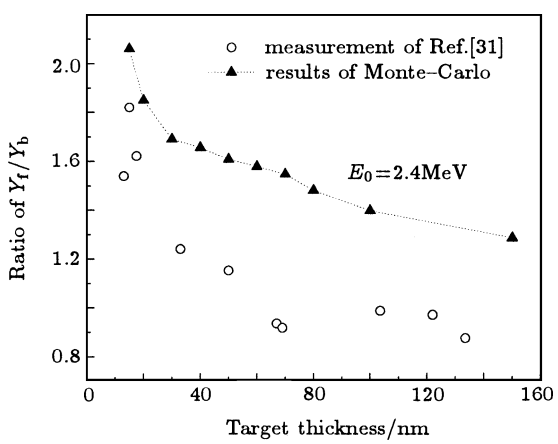


Fig.1. Ratio of the forward electron yield to the backward one, $Y_{\rm f}/Y_{\rm b}$, as a function of target thickness at the projectile energy E_0=2.4MeV.

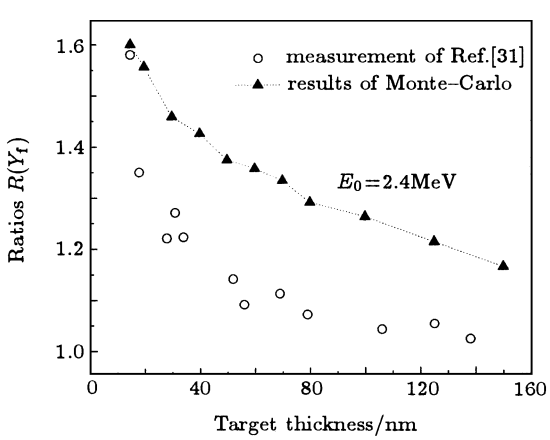


Fig.2. Ratio $R(Y_{\rm f})$ as a function of target thickness for the projectile energy E_0=2.4MeV.

The relationship between the backward electron emission yield $Y_b(\theta)$ and incident angle θ is $Y_b(\theta) = Y_b(0)\cos^{-f}\theta$. The calculated results of f are shown in Fig.3. f is about 0.85 except for f approximating to 1 near the $E_0 = 500$keV. Results shows $f \neq 1$, which means that Eq.(1) does not hold for H_2^+ bombardment. The calculated electron yield Y_b as a function of energy at $\theta = 0$ is shown in Fig.4. If $\Lambda = 0.135$ and λ_s=8nm are chosen, the result from Eq.(6) is in good agreement with that of simulation in the energy range considered. In Fig.5, we show the backward electron yield Y_b as a function of θ at the energies of E_0=500keV and E_0=3000keV, respectively. The results of simulation and those from Eq.(6) are also in good agreement with each other. According to these facts, it is readily to understand the reason why Eq.(1) does not hold for H_2^+ bombardment. In Eq.(6), we assume that Eq.(1) holds for the electron yield induced by H_2^+ and (H^++H^+)-proton-pairs, but actually it is not true for the stripped electron. The simulation results also prove the assumption. The calculated f of electron yield induced by H_2^+, (H^++H^+) and e^- is shown in Fig.6. We can see $f \approx 1$ for Y_1 and Y_2, and this is consistent with assumption in Eq.(6). But for Y_e, $f \approx 0.35$, it is much smaller than 1. The gained energy of the stripped electron is no more than 1 keV in the projectile energy range investigated. The trajectory of low energy electron is in a zigzag form duo to multiple collisions with target atoms. It causes the probability of the backscattered electrons escaping without generating secondary electrons to increase with the incident angle θ. So the total backward electron yield deviates from the inverse cosine law.

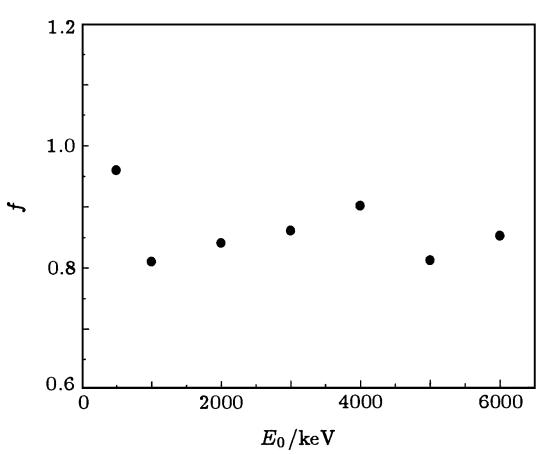


Fig.3. Calculated parameter f.

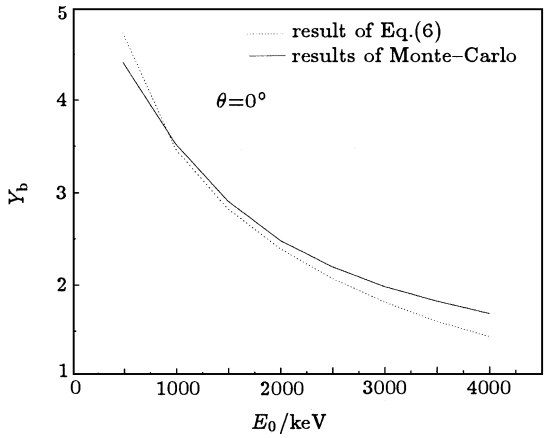


Fig.4. Backward electron emission yield Y_b as a function of projectile energy E_0.

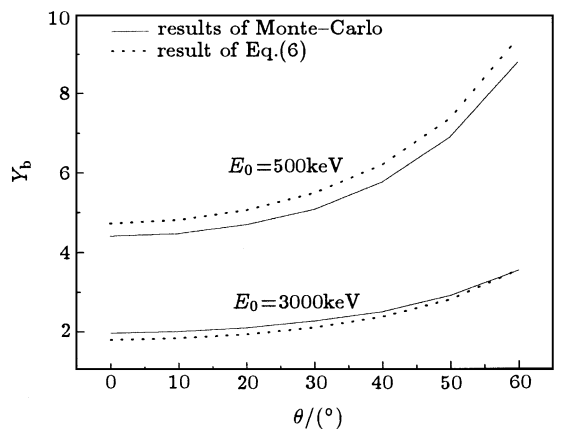


Fig.5. Backward electron emission yield Y_b as a function of incident angle θ.

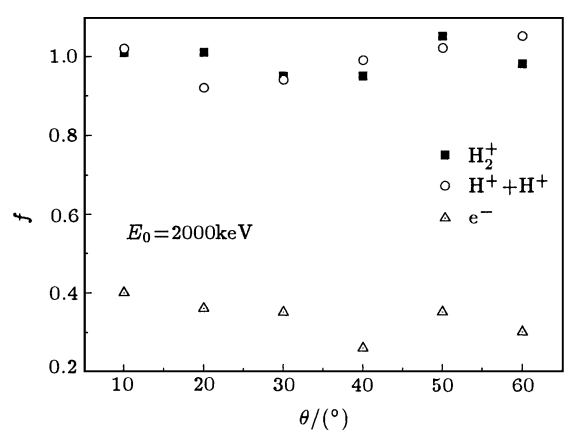


Fig.6. Parameter f of electron yield induced by H_2^+, (H^++H^+) and e^-, respectively.

Due to the increasing rate of $Y_b(\theta)$ being smaller than that of $Y_b(0)\cos^{-1}\theta$, the ratio of forward electron emission yield to backward one, Y_f/Y_b, at the inclining incidence is different from that at the normal incidence for an effective target thickness. The calculated result is given in Fig.7 at an energy of 3000keV.

The ratio decreases with the thickness at the normal incidence. For the thickness $D \geq$50nm, the backward electron yield is hardly changed with the thickness. The thicker the target is, the longer the dwell time of (H^++H^+) in the solid will be. The internuclear distance r increases near the exit interface of the target as the thickness increases for a given projectile velocity. But, accordingly, the effective charge $Z_{\rm eff2}$ decreases. The contribution of the stripped electrons to the forward emission yield is negligible for the thickness considered. So the ratio decreases with thickness. The similar results have been discussed above. We assume that the inverse cosine law holds true for the forward electron yield. Although the $Z_{\rm eff2}$ near the exit interface decreases with θ, the increasing rate of forward electron yield $Y_{\rm f}(\theta)$ will be somewhat lower than that of $Y_{\rm f}(0)\cos^{-1}\theta$. But little change of internuclear distance r of (H^++H^+) takes place for the thickness increasing from 50 to 100nm. Correspondingly, $Z_{\rm eff2}$ has the same trend as r. The increasing rate of $Y_{\rm f}(\theta)$ with θ is faster than that of $Y_{\rm b}(\theta)$. So the ratio of the forward electron emission yield to the backward one at inclining incidence will increase with θ.

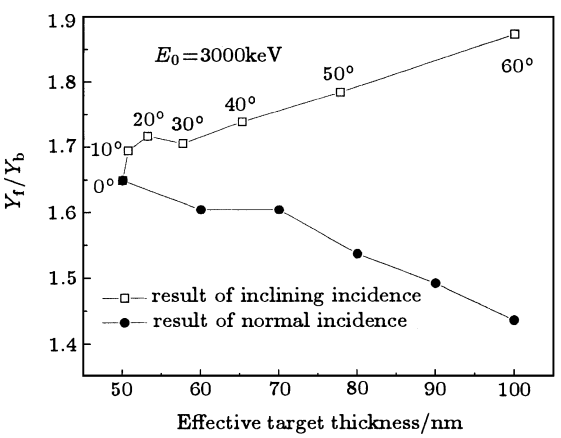


Fig.7. Ratio of the forward electron yield to the backward one, $Y_{\rm f}/Y_{\rm b}$, vs effective target thickness at the inclining and normal incidence.

5. Backward electron emission statistics

The distribution of the number of secondary electrons induced by per projectile ion is called electron emission statistics. Many authors have studied the topics theoretically and experimentally. The results show that the statistics does not fulfil the Poisson distribution

$$P_n(Y) = \frac{Y^n}{n!}{\rm e}^{-Y}. \qquad (13)$$

Here, Y is the mean value of the distribution which is equivalent to electron emission yield $Y_{\rm b}(\theta)$, and n is the number of secondary electrons induced by per projectile ion. For projectiles with low velocities ($v_0 < v_{\rm B}$, $v_{\rm B}$ is the Bohr velocity), the deviation from Poisson distribution mainly results from the large angle scattering of projectile ions and the recoiling of target atoms.[32–36] For ions with high velocities ($v_0 > v_{\rm B}$), the deviation is mainly due to electron cascade in the solid, and the distribution can be reproduced fairly well by the Pólya distribution[37–40]

$$P_{\rm n}(Y,b) = \frac{Y^n}{n!}(1+bY)^{-n-1/b}\prod_{i=1}^{n}[1+(i-1)b], \qquad (14)$$

where b is the deviation parameter from Poisson distribution.

In Refs.[37–40], the projectile is atomic ion and the incident angle is invariable. So we also calculate electron emission statistics induced by swift H_2^+. One of the results for the distribution is shown in Fig.8. According to the results, we find that the statistics can be described by Eq.(14). The value of b is independent of the incident angle and only increases with projectile energy. The calculated b as a function of E_0 is given in Fig.9. It is obvious that the cascade process of the excited electrons by projectile is almost independent of incident angle when θ is not large enough ($\theta < 60°$). The gained energy of some excited electrons increases with E_0, and their cascade becomes more important, so the deviation parameter b from the Poisson distribution increases with E_0.

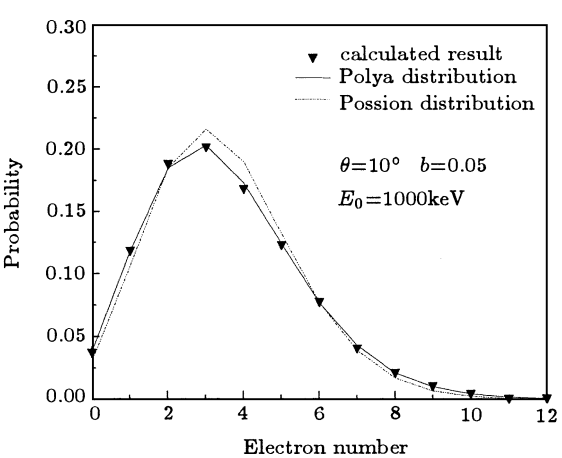


Fig.8. Electron emission statistics of projectile energy, when E_0=1000keV at $\theta = 10°$.

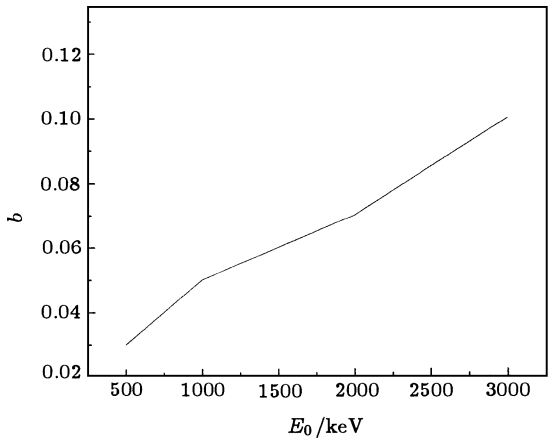


Fig.9. Parameter b as a function of projectile energy E_0.

6. Conclusion

The incident angle dependence of secondary electron emission induced by a swift H_2^+ ion incident on C is studied using the Monte Carlo method combined with the semiempirical theory. The results show that backward electron emission yield deviates from the inverse cosine law due to the effect of the valence electrons of H_2^+. The ratio of the forward electron emission yield to the backward one at the inclining incidence is different from that at the normal incidence. The electron emission statistical distribution is independent of the incident angle. The value of b, the deviation parameter from the Poisson distribution, increases with projectile energy.

References

[1] Benazeth N 1987 *J. Microsc. Spectrosc. Electron* **12** 235
[2] Svensson B and Holmén G 1981 *J. Appl. Phys.* **52** 6928
[3] Veje E 1981 *Radiat. Eff. Lett.* **58** 35
[4] Svensson B, Holmén G and Burén A 1981 *Phys. Rev.* B **24** 3749
[5] Ferron J, Alonso A V, Baragiola R A and Oliva-Florio A 1981 *Phys. Rev.* B **24** 4412
[6] Veje E 1984 *Nucl. Instrum. Meth.* B **2** 536
[7] Ohya K and Kawata J 1994 *Nucl. Instrum. Moth* B **90** 552
[8] Kawata J and Ohya K 1994 *Radiat. Eff. and Defect S.* **130-131** 552
[9] Kawata J, Ohya K and Mori I 1992 *Jpn. J. Appl. Phys.* part l **31** 2560
[10] Chauhan R S, Mittal V K, Naudi T K and Avasthi D K 1997 *Vacuum* **48** 1031
[11] Hesselkamp D in 1992 *Particle Induced Electron Emission II* ed Hohler G (Berlin: Springer) p1
[12] Ziegler J F and Manoyan J M 1988 *Nucl. Instrum. Meth.* B **35** 25
[13] Ogawa H, Sakamoto N and Tsuchida H 2000 *Nucl. Instrum. Meth.* B **164-165** 279
[14] Billebaud A, Fallavier M, Kirsch R, Poizat J C, Remillieux J and Vidović Z 1997 *Phys. Rev.* A **55** 1124
[15] Sternglass E J 1957 *Phys. Rev.* **108** 1
[16] Ziegler J F, Biersack J P and Littmark U 1985 *The Stopping and Range of Ion in Solids* (New York: Pergamon)
[17] Wang Y N and Ma T C 1993 *Phys. Lett.* A **178** 209
[18] Brandt W and Ratkowski A 1974 *Phys. Rev. Lett* **33** 1325
[19] Ohya K, Harada A, Kawata J and Nishimura K 1996 *Jpn. J. Appl. Phys.* **35** 6226
[20] Ono S and Kanaya K 1979 *J. Phys.* D: *Appl. Phys.* **12** 619
[21] Kawata J, Ohya K and Mori I 1992 *Jpn. J. Appl. Phys.* part l **31** 1453
[22] Ohya K, Kawata J and Mori I 1990 *Jpn. J. Appl. Phys.* **29** 1316
[23] Caron M *et al* 1998 *Nucl. Instrum. Meth.* B **135** 436
[24] Steinbauer E, Schinner A and Benka O 2000 *Nucl. Instrum. Methods* B **171** 291
[25] Lu Q L, Zhao G Q and Zhou Z Y 2003 *Acta Phys. Sin.* **52** 1278 (in Chinese)
[26] Zhang L Zh *et al* 2001 *Chin. Phys.* **10** 639
[27] Tan Z Y and Xia Y Y 2002 *Acta Phys. Sin.* **51** 1506 (in Chinese)
[28] Biersack J P and Haggmark L G 1980 *Nucl. Instrum. Methods* **174** 257
[29] Lu Q L, Zhao G Q and Zhou Zh Y 2002 *Nucl. Instrum. Methods* B **192** 267
[30] Liljequist D 1989 *J. Appl. Phys.* **65** 2431
[31] Kroneberger K, Clouvas A, Schlüssler G, Koschar P, Kemmler J, Rothard H, Biedermann C, Heil O, Burkhard M and Groeneveld K O 1988 *Nucl. Instrum. Methods* B **29** 621
[32] Ohya K and Mori I 1992 *Nucl. Instrum. Methods* B **67** 628
[33] Ohya K and Kawata J 1994 *Radiat. Eff. Defect S.* **130-131** 628
[34] Ohya K and Kawata J 1993 *Jpn. J. Appl. Phys.* part l **32** 1803
[35] Ohya K, Aumayr F and Winfer H 1992 *Phys Rev.* B **46** 3101
[36] Lakits G, Aumayr F and Winter H 1989 *Phys. Lett.* A **139** 395
[37] Steinbauer E, Schinner A and Benka O 2000 *Nucl. Instrum. Methods* B **171** 291
[38] Benka O, Fink T, Schinnner A and Steinbauer E 1997 *Nucl. Instrum. Methods* B **125** 41
[39] Benka O, Schinner A and Fink T 1995 *Phys. Rev.* A **51** 2281
[40] Azuma T, Yamazaki Y, Komaki K, Sekiguchi M, Hasegawa T, Hattori T and Kuroki K 1992 *Nucl. Instrum. Methods* B **67** 636